Evaluation of EGFR-targeted radioimmuno-gold-nanoparticles as a theranostic agent in a tumor animal model

ARTICLE *in* BIOORGANIC & MEDICINAL CHEMISTRY LETTERS · APRIL 2013

Impact Factor: 2.42 · DOI: 10.1016/j.bmcl.2013.04.002 · Source: PubMed

Bioorganic & Medicinal Chemistry Letters 23 (2013) 3180–3185

Contents lists available at SciVerse ScienceDirect

Bioorganic & Medicinal Chemistry Letters

journal homepage: www.elsevier.com/locate/bmcl

Evaluation of EGFR-targeted radioimmuno-gold-nanoparticles as a theranostic agent in a tumor animal model

Hao-Wen Kao [a,†], Yi-Yu Lin [a,†], Chao-Cheng Chen [a], Kwan-Hwa Chi [b], Der-Chi Tien [c], Chien-Chung Hsia [d], Ming-Hsien Lin [e], Hsin-Ell Wang [a,*]

[a] Department of Biomedical Imaging and Radiological Sciences, National Yang-Ming University, No. 155, Sec. 2, Linong St., Beitou District, Taipei 112, Taiwan, ROC
[b] Shin Kong Wu Ho-Su Memorial Hospital, Taipei, Taiwan, ROC
[c] Department of Mechanical Engineering, National Taipei University of Technology, Taipei, Taiwan, ROC
[d] Institute of Nuclear Energy Research, Taoyuan, Taiwan, ROC
[e] Taipei City Hospital Zhongxiao Branch, Taipei, Taiwan, ROC

ARTICLE INFO

Article history:
Received 13 February 2013
Revised 29 March 2013
Accepted 2 April 2013
Available online 10 April 2013

Keywords:
Gold nanoparticle
Epidermal growth factor receptor
Cetuximab
SPECT

ABSTRACT

This study evaluated the tumor targeting and therapeutic efficacy of a novel theranostic agent ^{131}I-labeled immuno-gold-nanoparticle (^{131}I-C225-AuNPs-PEG) for high epidermal growth factor receptor (EGFR)-expressed A549 human lung cancer. Confocal microscopy demonstrated the specific uptake of C225-AuNPs-PEG in A549 cells. ^{131}I-C225-AuNPs-PEG induced a significant reduction in cell viability, which was not observed when incubated with AuNPs-PEG and C225-AuNPs-PEG. MicroSPECT/CT imaging of tumor-bearing mice after intravenous injection of ^{123}I-C225-AuNPs-PEG revealed significant radioactivity retention in tumor suggested that ^{131}I-labeled C225-conjugated radioimmuno-gold-nanoparticles may provide a new approach of targeted imaging and therapy towards high EGFR-expressed cancers.

Despite decades of research in the biology and treatment of cancer, it remains major leading cause of death worldwide. Tumor heterogeneity and adaptive resistance remain formidable challenges to therapy. Researchers have recently begun to engineer multifunctional nanoparticles with properties suitable for both imaging and treatment of cancer in an effort to better manage the disease. Among the inorganic nanoparticles, gold nanoparticle (AuNP) has been used clinically as a contrast agent for CT imaging.[1] Gold nanoparticle is widely applied because of its bioinert, nontoxic, and readily synthesized and functionalized characteristics. [2] It can passively target tumor sites by the enhanced permeability and retention (EPR) effect in neoplasm lesions.[1,3] To date, four different types of gold nanoparticles have been tested in a preclinical setting as contrast agents for molecular imaging: nanospheres, nanocages, nanorods and nanoshells.[4,5] To achieve further accumulation of nanoparticles in the tumor cell and enhancement of the efficiency by specific endocytosis, various surface modifications of nanoparticles with active ligands were developed. This phenomenon is commonly referred to as active targeting, which combine with passive targeting to achieve the maximum localization of nanoparticles in malignant tissues.[6,7] Since the strong and selective interaction of sulfur groups for gold, the sulfur containing targeting ligands chemisorbed to the nanoparticle surface through the sulfur bond were used.[8]

Epidermal growth factor receptor (EGFR) is a cell surface receptor which plays key role in signaling pathways that regulate cell proliferation, angiogenesis and tumor metastases.[9,10] This receptor was widely overexpressed in several tumor types including breast cancer, melanoma, and brain glioblastoma, making EGFR an attractive candidate for anti-cancer therapy.[11,12] Recent reports of EGFR targeting strategies have involved the use of anti-EGFR antibodies to block EGF binding to the receptor or as a targeting ligand for the delivery of therapeutic agents.[13] Cetuximab (Erbitux®, C225), a recombinant human/mouse chimeric monoclonal antibody that binds specifically to the extracellular domain of the human EGFR, was approved by Food and Drug Administration in 2004 as a second-line treatment of advanced colorectal cancer.[14] Bound antibody with high affinity competitively inhibits the binding of epidermal growth factor (EGF) with EGFR, thereby preventing downstream signal transduction. Cetuximab as a promising therapeutic agent has been applied for the treatment of EGFR-expressing malignant tumors in preclinical studies and clinical trials, mainly in combination with chemo-[15,16] or radio-therapy.[17,18] Glazer et al. have reported that C225 conjugated gold nanoparticles (C225-AuNPs) induced significant tumor destruction in a murine model of pancreatic carcinoma after radio-frequency (RF) field exposure.[19]

* Corresponding author. Tel.: +886 2 28267215; fax: +886 2 28201095.
E-mail address: hewang@ym.edu.tw (H.-E. Wang).
† These authors contributed equally to this work.

0960-894X/$ - see front matter © 2013 Elsevier Ltd. All rights reserved.
http://dx.doi.org/10.1016/j.bmcl.2013.04.002

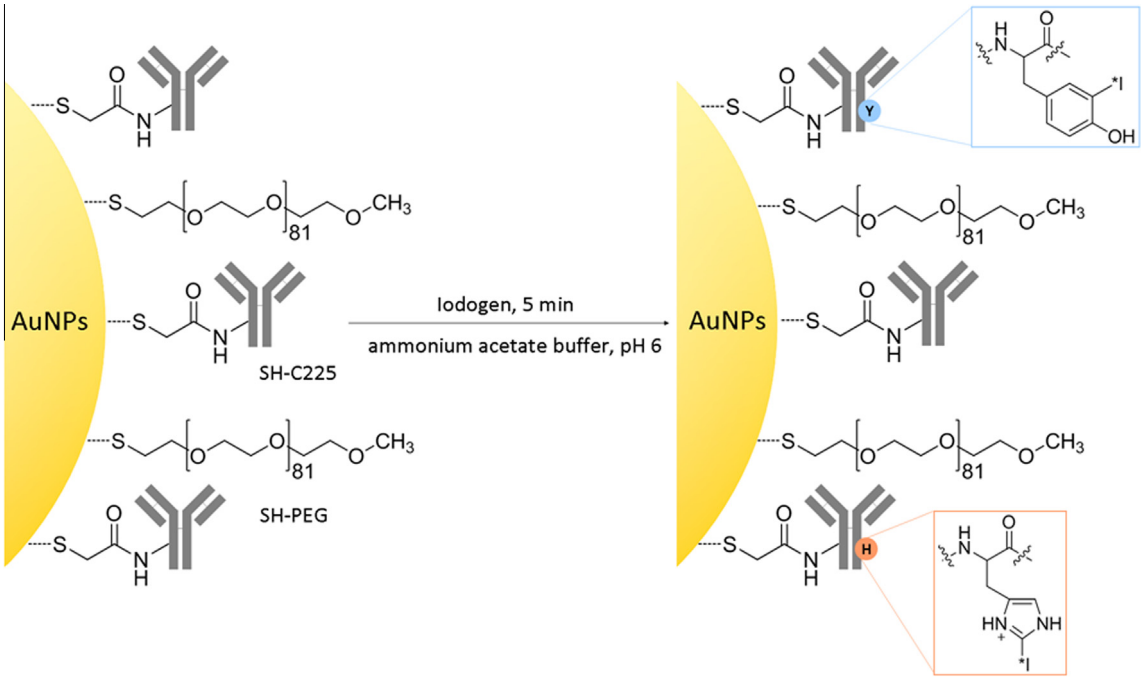

Figure 1. Scheme of radioiodination of C225-AuNPs-PEG using iodogen method.

Targeted radionuclide therapy and radioimmunotherapy (RIT) are in the forefront of molecular cancer treatment modalities that involve the use of cancer cell targeting radiopharmaceuticals, such as radiolabeled antibodies.[20,21] With RIT, the radiation is delivered not only to the antibody-bound tumor cell, but also to the neighboring non-antibody-bound tumor cells through the 'cross-fire' effect, complying with the path length of the radioactive isotope. Iodine-131 ($t_{1/2}$ = 8.01 days), a radionuclide with a gamma emission of 364 keV (81.7%) and a beta emission of 0.606 MeV (89.9%), provides imaging feasibility and beta-emitting therapeutic effect. In this study, a potent theranostic agent for radioimmunotherapy, ^{131}I-C225-AuNPs-PEG, was successful synthesized (Fig. 1). The enhanced endocytosis and cytotoxicity of ^{131}I-C225-AuNPs-PEG to high EGFR-expressed human A549 lung carcinoma cells, and active targeting to A549 tumor xenograft in a mouse model, were demonstrated.

Gold nanoparticles (AuNPs) were prepared using citrate reduction of chloroauric acid ($HAuCl_4$) following the methods described in literature.[22] C225 (10 μg/mL) modified with free sulfhydryl group was conjugated with AuNPs suspension (10×10^{10} particles/mL) at pH 8 for 1 h at ambient temperature. Polyethylene glycol-SH was added to the mixture up to a final concentration of 0.2 mg/mL, and the solution was centrifuged to remove unbound antibodies and PEG. The surface plasmon resonance spectra recorded on a Jasco V-530 UV/vis spectrophotometer showed an 8-nm red shift in the plasmon peak (λ_{max}) of the antibody-conjugated gold nanoparticles (Fig. 2A), indicating a successful conjugation of antibodies to AuNPs without aggregation. The particle size and size distribution of bare AuNPs and C225-AuNPs-PEG were determined by dynamic light scattering method using a Zetasizer Nano ZS (Malvern, Worcestershire, UK). The average particle size was 25.7 nm for bare AuNPs and 52.9 nm for C225-AuNPs-PEG, revealed that a layer of antibody molecules of ~13.6 nm was coated over the gold nanoparticles (Fig. 2B). The monomodal distribution and the TEM images suggested that the particles remain well dispersed as single entities and do not form agglomerates.

Sodium dodecyl sulfate–polyacrylamide gel electrophoresis (SDS–PAGE) combined with PageBlue™ Protein staining (Fermentas, Vilnius, Lithuania) is used to evaluate the average number of C225 molecules present on each gold nanoparticle. A serial dilution of C225 (0–4 μg) was conducted to construct a calibration curve for the determination of conjugated C225. As shown in Fig. 2C, lane 2 was a molecular marker. Lane 3, bare AuNPs, showed no protein bands and served as a negative control. The C225-conjugated AuNPs loaded in lane 4 also showed the same two bands (26- and 51-kDa) as that observed while loading C225 standard (lane 1). Each gold nanoparticle was estimated conjugated with about 124 antibody molecules. Chattopadhyay et al. have reported that gold nanoparticles exhibit apparent light absorption covering a wide range of visible and UV wavelengths.[23] When conjugated with C225, the high background absorption owing to the gold nanoparticles may hinder accurate determination of the bound proteins by standard colorimetric methods (e.g., bicinchoninic acid assay and Bio-Rad protein assay). In our study, conjugated antibodies were first separated from the gold nanoparticles by SDS–PAGE, and then quantitative determination by using Coomassie blue staining was conducted to overcome the previous problem.[24]

To investigate the stability of C225-AuNPs-PEG in PBS (4 °C) and fetal bovine serum (FBS, 37 °C), the time-dependent absorbance spectra of the incubated specimen were recorded.[25] The consistent absorbance and λ_{max} of C225-AuNPs-PEG PBS incubation at designated time points (0, 0.5, 1, 2, 4, 8, and 24 h at 4 °C, Fig. 3) displayed the stability of C225-AuNPs-PEG in PBS. In FBS at 37 °C, the absorbance and λ_{max} of the incubation declined slightly and shifted less than 1 nm after a 24-h incubation, implied that C225-AuNPs-PEG remained well dispersed in plasma.

Gold nanoparticle, as a fluorescent probe, has been used for fluorescence imaging after incubation with HeLa cells.[26] The specific targeting and internalization of C225-AuNPs-PEG into tumor cells were assessed by confocal fluorescence microscopy. A non-uniform distribution of red fluorescence emissions in the cytoplasm indicated internalization of C225-AuNPs-PEG in A549 cells (Fig. 4A). No fluorescence emission was found within the nuclei. Chang et al. have reported that gold nanoparticles visualized by silver enhancement co-localized with endoplasmic reticulum and Golgi after incubation with B16F10 melanoma cells.[27] For blocking

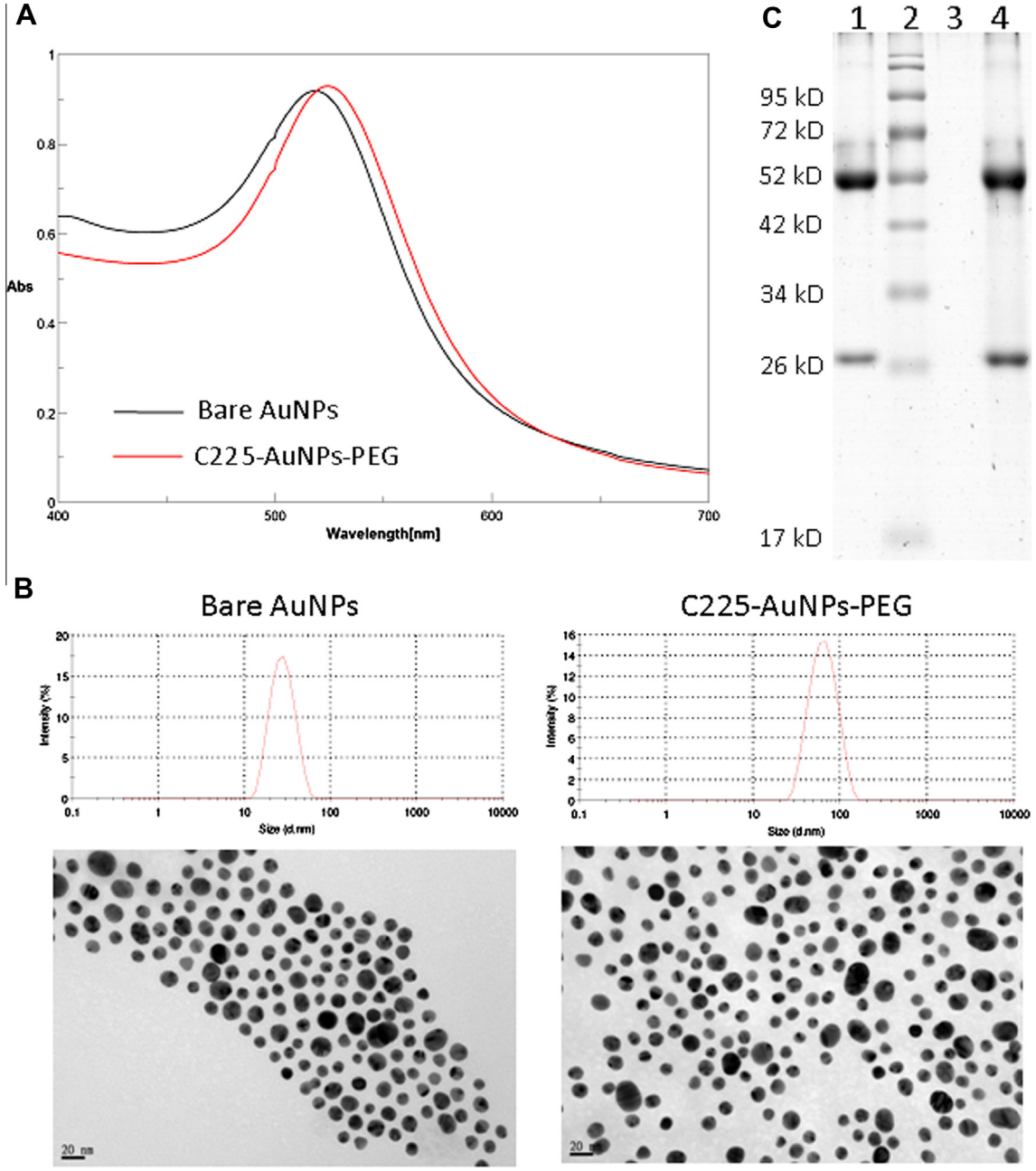

Figure 2. (A) The peak plasmonic absorbance of the cetuximab-conjugated gold nanoparticles (C225-AuNPs-PEG, 52.9-nm, red) displayed appreciable shift from that of the bare AuNPs (25.7-nm, black). (B) Size distribution of AuNPs (left) and C225-AuNPs-PEG (right) was analyzed by dynamic light scattering and TEM imaging. (C) Photograph of the gel after Coomassie blue staining. Lane 1, C225 only; lane 2, molecular marker; lane 3, AuNPs only (negative control); lane 4, C225-AuNPs-PEG. In lane 1 and lane 3, two strong bands at 26 and 51 kDa were detected.

experiments, a 200-fold excess of C225 was added into the A549 incubation to saturate the binding sites of EGFR for 1 h, and then C225-AuNPs-PEG were added. The fluorescence emission in A549 cells was efficiently retarded (Fig. 4B), demonstrated that C225-AuNPs-PEG displayed specific binding to EGF receptors.

Cetuximab labeled with different radioisotopes, for example, ^{90}Y and ^{177}Lu, are of potential use in radioimmunotherapy as a treatment regimen for EGFR-overexpressed tumors.[28,29] In the present study, C225-AuNPs-PEG were labeled with $^{123/131}$I ($Na^{131}I$, Nuclear Science and Technology Development Center, National Tsing-Hua University, Hsinchu, Taiwan; $Na^{123}I$, Institute of Nuclear Energy Research, Taoyuan, Taiwan) using the Iodogen method.[30] $^{123/131}$I-C225-AuNPs-PEG were prepared with moderate radiochemical yield (about 30%) and high radiochemical purity (>95%) determined by ITLC-SG (Varian Inc.) using normal saline as the mobile phase. For in vitro stability study, ^{131}I-C225-AuNPs-PEG preparation (3×10^{11} particles/mL, 148 MBq/mL) was incubated in PBS at 4 °C and in FBS (in a 1:10 volume ratio) at 37 °C. The radiochemical purity was >85% in PBS at 4 °C and was ~50% in FBS at 37 °C after a 48-h incubation.

Several researchers have reported that gold nanoparticle displayed good biocompatibility in types of malignant cells and normal cells.[2] In this study, the cytotoxicity of ^{131}I-C225-AuNPs-PEG in A549 cells was assessed by MTT assay. Four formulations of gold nanoparticle conjugates (AuNPs-PEG, C225-AuNPs-PEG, ^{131}I-C225-AuNPs-PEG, ^{131}I-C225-AuNPs-PEG plus a 200-fold excess of C225, and ^{131}I-iodide as the control) at various concentrations (ranged from 0 to 0.625 μg/mL of AuNPs) were added to the wells,

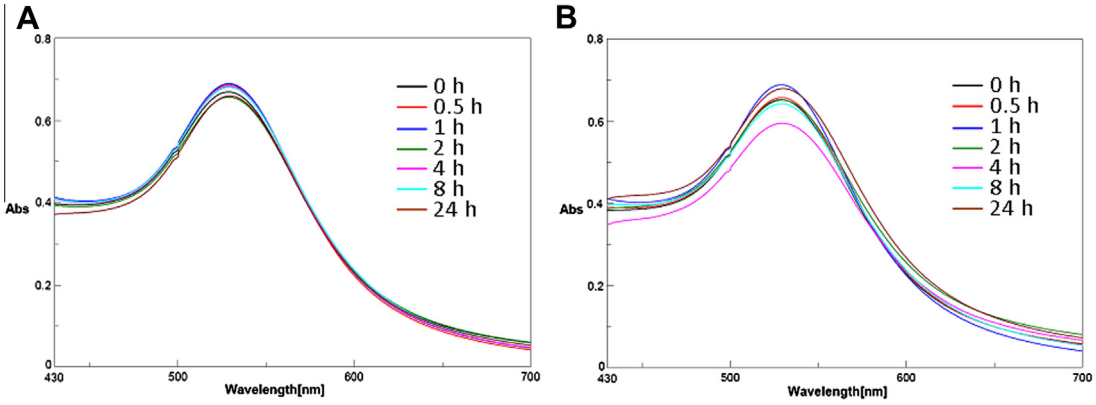

Figure 3. UV–vis spectra of C225-AuNPs-PEG after incubation in PBS (4 °C, A) and FBS (37 °C, B) for various periods of time indicated good in vitro stability within 24 h.

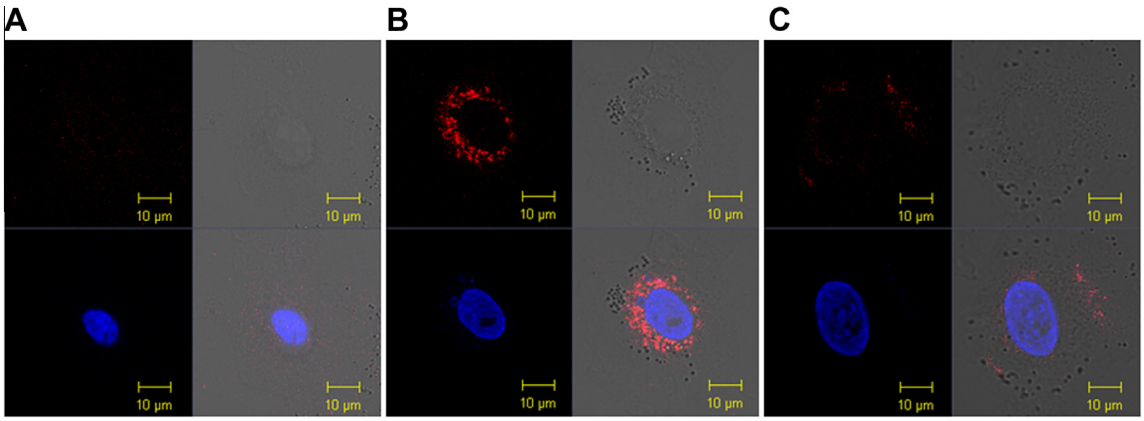

Figure 4. Confocal microscopy images of A549 cells after incubation for 30 min in PBS (control, A), with C225-AuNPs-PEG (2×10^9 particles/mL, B), and with C225-AuNPs-PEG in the presence of a 200-fold excess of C225 to block EGF receptors (C) revealed specific uptake and internalization of C225-AuNPs-PEG in high EGFR-expressed cells. The cell nucleus was visualized with DAPI (blue).

incubated for 2 h at 37 °C, then replaced with fresh medium and incubated for another 24 h. Non-radioactive gold nanoparticles, AuNPs-PEG and C225-AuNPs-PEG, exhibited good biocompatibility at concentrations up to 0.625 μg/mL, while ^{131}I-C225-AuNPs-PEG (ranged from 0 to 0.625 μg/mL of AuNPs, 0 to 185 kBq/mL of ^{131}I) exhibited appreciable and dose-dependent cytotoxicity compared with that of its non-radioactive counterpart (Fig. 5A). At the maximal dosage (0.625 μg/mL of AuNPs, 185 kBq/mL of ^{131}I), the viability of ^{131}I-C225-AuNPs-PEG treated A549 cells dropped to approximately 37%, while that of the blocking group (pretreated with a 200-fold excess of C225) and the control group (treated with ^{131}I-iodide) was both higher than 82% (Fig. 5). The findings suggested that ^{131}I-C225-AuNPs-PEG is a promising radioimmuno theranostic agent for the treatment of high EGFR-expressed tumor cells.

Gold nanoparticle, which could induce acceleration in the G0/G1 phase and increased the population of cells in the G2/M phase, was recently conceived as a potent radiosensitizer. Compared to X-rays alone, glucose-capped gold nanoparticle showed a 1.5–2.0 fold

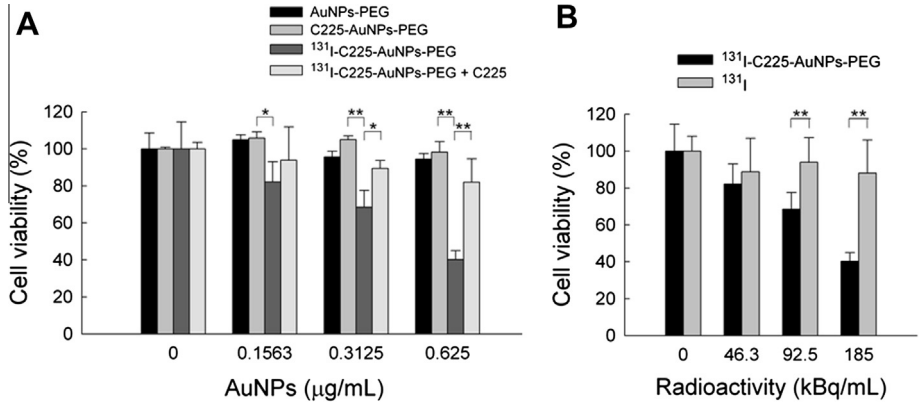

Figure 5. In vitro cell viability measured by MTT assays. (A) A549 cells were incubated with various concentrations of AuNPs-PEG (0.0–0.625 μg/mL), C225-AuNPs-PEG (0.0–0.625 μg/mL) and ^{131}I-C225-AuNPs-PEG (0.0–0.625 μg/mL, 0.0–185 kBq/mL) for 2 h and then 24 h in fresh medium. Both AuNPs-PEG and C225-AuNPs-PEG showed high biocompatibility, while ^{131}I-C225-AuNPs-PEG displayed significant cytotoxicity. (B) Comparison between ^{131}I-C225-AuNPs-PEG (0 to 185 kBq/mL) and ^{131}I (0–185 kBq/mL) on A549 cells. $^{*}p$ <0.05; $^{**}p$ <0.01.

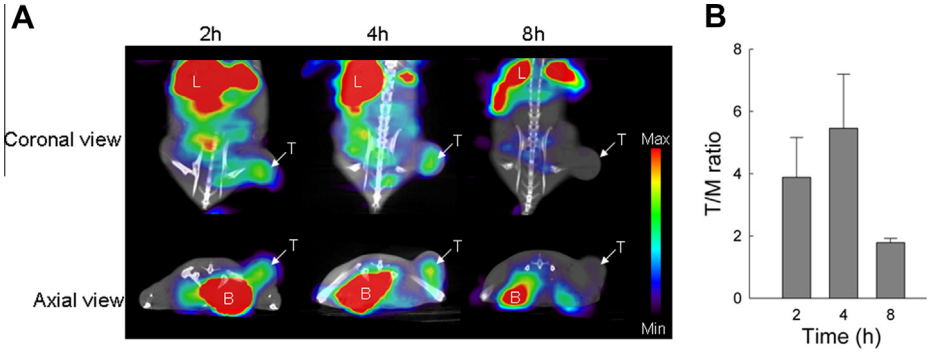

Figure 6. (A) MicroSPECT/CT images of A549 tumor-bearing mice at 2, 4 and 8 h after intravenous injection of 18.5 MBq of ^{123}I-C225-AuNPs. The mice were anesthetized with 1% isoflurane (w/v) in oxygen in the prone position. Tumor nodules are indicated by arrow. T, tumor; L, liver; B, bladder. (B) Tumor-to-muscle ratios derived from microSPECT images.

enhancement in growth inhibition in DU-145 cancer cell.[31] Chang et al. reported that gold nanoparticle in conjunction with 6 MeV electron beam irradiation significantly increased the apoptotic signals, retarded the tumor growth and prolonged the mean survival time compared to irradiation alone in a B16F10 tumor-bearing mouse model.[27] In this study, a concurrent display of internal irradiation from labeled ^{131}I-radionuclide and the intrinsic radiosensitization effect of ^{131}I-C225-AuNPs-PEG may account for the significant reduction in A549 cell viability after treatment. However, the in vivo therapeutic efficacy and the mechanism of ^{131}I-C225-AuNPs-PEG in cancer treatment need further investigations.

At 4 weeks after A549 cells inoculation, the tumor grows to about 150 mm^3 then animal imaging was conducted after intravenous injection of ^{123}I-C225-AuNPs-PEG (18.5 MBq) using a microSPECT/CT scanner (FLEX Triumph Regular FLEX X-OCT, Northridge, California, USA). Animal protocols were approved by the Institutional Animal Care and Use Committee (IACUC) of National Yang-Ming University (Taipei, Taiwan). The static images were acquired for 30 min at 2, 4 and 8 h post injection. Clear tumor uptake can be observed within 4 h post injection in the coronal and transaxial images (Fig. 6A). The tumor-to-muscle ratio was 3.9 and 5.5 at 2 and 4 h post injection (Fig. 6B). Liver and spleen, the reticuloendothelial system-rich organs, exhibited significant uptake of nano-sized particulate radiotracer. The remarkable accumulation in bladder implied that renal clearance was the predominant route of excretion of radioactive metabolites. A glutathione-coated luminescent gold nanoparticle (3 nm diameter)[32] and a gadolium-loaded dendrimer-entrapped gold nanoparticle (90 nm mean diameter)[33] have been reported to excrete via urinary system.

The experimental procedures are detailed in 'References and notes'.[34–36]

In conclusion, conjugation of monoclonal antibody cetuximab to gold nanoparticles and then labeled with I-131 to prepare ^{131}I-C225-AuNPs-PEG were successfully achieved. As a novel radioimmuno theranostic agent, ^{131}I-C225-AuNPs-PEG exhibited pronounced anti-proliferation ability to high EGFR-expressed cancer cells and clear tumor imaging in an A549 human lung carcinoma-xenografted mouse model.

Acknowledgments

This study was supported by Grants from the Department of Health, Taipei City Government, Taiwan (10201-62-066) and Institute of Nuclear Energy Research, Taiwan. We thank the Taiwan Mouse Clinic which is funded by the National Research Program for Biopharmaceuticals (NRPB) at the National Science Council (NSC) of Taiwan for technical support in microSPECT/CT experiment. The technical support in part by the Electron Microscopy Facility and the Imaging Core Facility of Nanotechnology in National Yang-Ming University is also gratefully acknowledged.

References and notes

1. Cho, E. C.; Glaus, C.; Chen, J.; Welch, M. J.; Xia, Y. *Trends Mol. Med.* **2010**, *16*, 561.
2. Lewinski, N.; Colvin, V.; Drezek, R. *Small* **2008**, *4*, 26.
3. Lim, Z. Z.; Li, J. E.; Ng, C. T.; Yung, L. Y.; Bay, B. H. *Acta Pharmacol. Sin.* **2011**, *32*, 983.
4. Murphy, C. J.; Gole, A. M.; Stone, J. W.; Sisco, P. N.; Alkilany, A. M.; Goldsmith, E. C.; Baxter, S. C. *Acc. Chem. Res.* **2008**, *41*, 1721.
5. Skrabalak, S. E.; Chen, J.; Sun, Y.; Lu, X.; Au, L.; Cobley, C. M.; Xia, Y. *Acc. Chem. Res.* **2008**, *41*, 1587.
6. Conde, J.; Doria, G.; Baptista, P. *J. Drug Deliv.* **2012**, *2012*, 751075.
7. Ghosh, P.; Han, G.; De, M.; Kim, C. K.; Rotello, V. M. *Adv. Drug Deliv. Rev.* **2008**, *60*, 1307.
8. Hakkinen, H. *Nat. Chem.* **2012**, *4*, 443.
9. Waksal, H. W. *Cancer Metastasis Rev.* **1999**, *18*, 427.
10. Citri, A.; Yarden, Y. *Nat. Rev. Mol. Cell Biol.* **2006**, *7*, 505.
11. Sharma, S. V.; Bell, D. W.; Settleman, J.; Haber, D. A. *Nat. Rev. Cancer* **2007**, *7*, 169.
12. Sharafinski, M. E.; Ferris, R. L.; Ferrone, S.; Grandis, J. R. *Head Neck* **2010**, *32*, 1412.
13. Zeineldin, R.; Muller, C. Y.; Stack, M. S.; Hudson, L. G. *J. Oncol.* **2010**, *2010*, 414676.
14. Graham, J.; Muhsin, M.; Kirkpatrick, P. *Nat. Rev. Drug Disc.* **2004**, *3*, 549.
15. Xiong, H. Q.; Rosenberg, A.; LoBuglio, A.; Schmidt, W.; Wolff, R. A.; Deutsch, J.; Needle, M.; Abbruzzese, J. L. *J. Clin. Oncol.* **2004**, *22*, 2610.
16. Van Cutsem, E.; Kohne, C. H.; Hitre, E.; Zaluski, J.; Chang Chien, C. R.; Makhson, A.; D'Haens, G.; Pinter, T.; Lim, R.; Bodoky, G.; Roh, J. K.; Folprecht, G.; Ruff, P.; Stroh, C.; Tejpar, S.; Schlichting, M.; Nippgen, J.; Rougier, P. *N. Eng. J. Med.* **2009**, *360*, 1408.
17. Dittmann, K.; Mayer, C.; Rodemann, H. P. *Radiother. Oncol.* **2005**, *76*, 157.
18. Gerber, D. E.; Choy, H. *Cancer Metastasis Rev.* **2010**, *29*, 171.
19. Glazer, E. S.; Zhu, C.; Massey, K. L.; Thompson, C. S.; Kaluarachchi, W. D.; Hamir, A. N.; Curley, S. A. *Clin. Cancer Res.* **2010**, *16*, 5712.
20. Kaminski, M. S.; Zasadny, K. R.; Francis, I. R.; Milik, A. W.; Ross, C. W.; Moon, S. D.; Crawford, S. M.; Burgess, J. M.; Petry, N. A.; Butchko, G. M., et al *N. Eng. J. Med.* **1993**, *329*, 459.
21. Bennett, J. M.; Kaminski, M. S.; Leonard, J. P.; Vose, J. M.; Zelenetz, A. D.; Knox, S. J.; Horning, S.; Press, O. W.; Radford, J. A.; Kroll, S. M.; Capizzi, R. L. *Blood* **2005**, *105*, 4576.
22. Frens, G. *Nat. Phys. Sci.* **1973**, *241*, 20.
23. Chattopadhyay, N.; Cai, Z.; Pignol, J. P.; Keller, B.; Lechtman, E.; Bendayan, R.; Reilly, R. M. *Mol. Pharm.* **2010**, *7*, 2194.
24. Dong, W. H.; Wang, T. Y.; Wang, F.; Zhang, J. H. *PLoS ONE* **2011**, *6*, e22394.
25. Zhang, X. D.; Wu, D.; Shen, X.; Chen, J.; Sun, Y. M.; Liu, P. X.; Liang, X. J. *Biomaterials* **2012**, *33*, 6408.
26. He, H.; Xie, C.; Ren, J. *Anal. Chem.* **2008**, *80*, 5951.
27. Chang, M. Y.; Shiau, A. L.; Chen, Y. H.; Chang, C. J.; Chen, H. H.; Wu, C. L. *Cancer Sci.* **2008**, *99*, 1479.
28. Niu, G.; Sun, X.; Cao, Q.; Courter, D.; Koong, A.; Le, Q. T.; Gambhir, S. S.; Chen, X. *Clin. Cancer Res.* **2010**, *16*, 2095.
29. Perk, L. R.; Visser, G. W.; Vosjan, M. J.; Stigter-van Walsum, M.; Tijink, B. M.; Leemans, C. R.; van Dongen, G. A. *J. Nucl. Med.* **2005**, *46*, 1898.
30. G.T. Hermanson, Bioconjugate Techniques, 2nd ed., Elsevier Inc., Nweyork, Academic Press: Amsterdam, 2008.
31. Roa, W.; Zhang, X.; Guo, L.; Shaw, A.; Hu, X.; Xiong, Y.; Gulavita, S.; Patel, S.; Sun, X.; Chen, J.; Moore, R.; Xing, J. Z. *Nanotechnology* **2009**, *20*, 375101.
32. Zhou, C.; Hao, G.; Thomas, P.; Liu, J.; Yu, M.; Sun, S.; Oz, O. K.; Sun, X.; Zheng, J. *Angew. Chem., Int. Ed.* **2012**, *51*, 10118.

33. Wen, S.; Li, K.; Cai, H.; Chen, Q.; Shen, M.; Huang, Y.; Peng, C.; Hou, W.; Zhu, M.; Zhang, G.; Shi, X. *Biomaterials* **2013**, *34*, 1570.

34. *Preparation and characterization of C225-AuNPs-PEG*: C225 (1.0 mg, 6.58 nmol, 2 mg/mL) was modified with *N*-succinimidyl S-acetylthioacetate (SATA, 15.2 μg, 65.7 nmol) for 1 h at ambient temperature and purified by passing through a Sephadex G50 column. SATA-modified C225 (1 mL, 400 μg/mL) was treated with hydroxylamine (200 μL, 0.5 M) at ambient temperature for 2 h. After passing through a Sephadex G50 column, C225 containing free sulfhydryl group (10 μg/mL) was conjugated with AuNPs suspension (10×10^{10} particles/mL) at pH 8 for 1 h at ambient temperature. Polyethylene glycol-SH (PEG-SH, mean molecular weight 5000, NOF Corporation, Japan) was added to the mixture up to a final concentration of 0.2 mg/mL. The solution was centrifuged at 3000 rpm for 30 min and the resulting pellet was washed twice with deionized water to remove unbound antibodies. After the third wash, the pellet was resuspended in PBS and stored at 4 °C until further use.
35. *Estimation of C225 number on AuNP:* The amount of antibody conjugated to AuNPs was estimated by sodium dodecyl sulfate polyacrylamide gel electrophoresis (SDS–PAGE). A series of C225 (range from 6.25 to 400 ng) was used to construct the standard curve. After reducing agent DTT was added to the sample, the samples were heated in a boiled water bath for 10 min. Each sample was loaded on a 10% SDS–PAGE. After electrophoresis, the gel was stained with PageBlue™ Protein Staining Solution (Fermentas, Vilnius, Lithuania), photographed using LAS-4000 mini image analyzer system (Fujifilm, Tokyo, Japan) and analyzed with the ImageJ program.
36. *Imaging of EGF receptor-mediated endocytosis by confocal microscopy:* One day before the experiment, A549 cells were seeded at a density of 2×10^5 cells per well into 6-well plates containing collagen-coated glass cover slips. After overnight incubation, the cells were incubated with C225-AuNPs-PEG (2×10^9 particles/mL) in serum free Ham's F12k medium at 37 °C for 30 min in a humidified CO_2 atmosphere (5%, v/v). After C225-AuNPs-PEG incubation, the medium was removed and washed three times with PBS and then fixed with 4% paraformaldehyde in PBS for 10 min at room temperature. After fixation, cell nuclei were stained with DAPI. The cover slips were washed abundantly with PBS and mounted upside down. For blocking experiment, cells were incubated with a 200-fold excess of C225 for 1 h prior to incubation with C225-AuNPs-PEG. Images of fixed cells were acquired on a laser scanning confocal system (ZEISS LSM 700; Zeiss, Oberkochen, Germany). Excitation was at 364 and 543 nm for visualization of DAPI and AuNPs, using 385–470 nm and 580–630 nm emission filter, respectively.